Rectangularly Driven Class-A Harmonic-Control Amplifier

Bernhard Ingruber, *Student Member, IEEE*, Josef Baumgartner, Dieter Smely, Martin Wachutka, *Student Member, IEEE*, Gottfried Magerl, *Member, IEEE*, and Felix A. Petz

***Abstract*— A rectangularly driven class-A harmonic-control amplifier (rHCA) is studied, which combines the advantage of high device drain efficiency (η_D) of a switched-type amplifier with the advantage of high gain (G) of class-A operation, thus maximizing its power-added efficiency (PAE). In this rHCA, harmonics are controlled such that drain-to-source voltage becomes half-sinusoidal. This reduces the necessary supply voltage without degrading output power. In comparison with a class-F amplifier using the same transistor, the realization of such an rHCA has demonstrated 0.4-dB larger output power, 3.8-dB increased gain, 4% higher PAE, and 22% lower drain supply voltage at 1.62 GHz.**

***Index Terms*—Harmonic control, high efficiency, high gain, low voltage, linearity, power amplifier.**

I. Introduction

ONE OF THE most critical aspects of mobile-communication equipment is dc power consumption. As the output power stage requires a major part of the total dc power, the key to solve this problem is high power-added efficiency (PAE) of this amplifier stage. Additionally, the reduction of supply voltage reduces mass and size of such handheld terminals. Modern communication systems employ modulation schemes that exhibit nonunity peak-to-average power ratio. As linearity of the power amplifier usually dominates the overall linearity of a transmitter, the power stage also has to provide low intermodulation distortion.

Today, class-F amplification is state-of-the-art in achieving high efficiency. This switched-type amplifier is driven at a class-B near input level, and with a special control of harmonics at its output, drain-to-source voltage becomes rectangular and drain current half-sinusoidal [see Fig. 1(a)]. Several researchers have concluded that even higher efficiency can be observed using a quasi-rectangular input signal to drive such a class-F amplifier [1]–[6]. All these amplifiers are distinguished by low intermodulation distortion, even at saturation where they offer high efficiency (see [7]–[11] and [4]–[6], respectively). In [9], it is reported on a conventional class-F amplifier that offers -23 dBc third-order intermodulation distortion distance at a drive level where its single-carrier PAE is 61%. The rectangularly driven class-F amplifier described in [5] delivers -25 dBc and 65%, respectively.

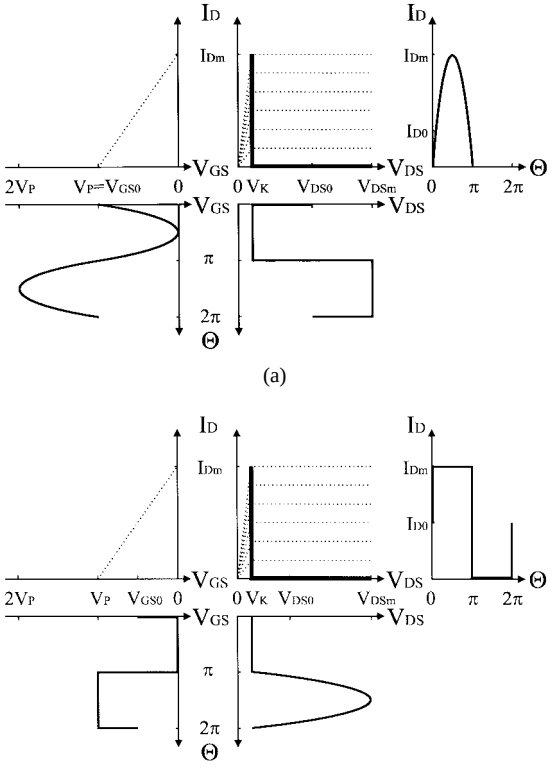

Fig. 1. Input and output characteristics of an idealized FET, gate and drain voltage and current waveforms, and dynamic load line (a) for class-F operation (b) of an rHCA.

The main disadvantage of such amplifiers is the gain loss due to an input bias near pinchoff [see Fig. 1(a)]. This lowers PAE, as

$$\mathrm{PAE} = \eta_D\left(1 - \frac{1}{G}\right). \tag{1}$$

Recently, we reported on an innovative amplifier concept where we used a half-sinusoidal signal to drive a class-F power-amplifier stage [12]. Due to class-A bias, gain could be increased by about 3 dB, as compared with a conventional class-F amplifier and, consequently, PAE was 3% higher.

Manuscript received October 11, 1997; revised June 10, 1998. This work was supported by the Austrian National Science Foundation (Fonds zur Förderung der wissenschaftlichen Forschung) under FWF Project P11422-OePY.

B. Ingruber, J. Baumgartner, D. Smely, and G. Magerl are with the Department of Electronic Design and Measurement Techniques, Vienna University of Technology, A-1040 Vienna, Austria.

M. Wachutka is with UTA Telecom AG, A-1090 Vienna, Austria.

F. A. Petz is with the European Space Agency (ESA-ESTEC), Noordwijk, The Netherlands.

Publisher Item Identifier S 0018-9480(98)08027-2.

In this paper, we present an additional class-A harmonic-control amplifier, which is driven by a quasi-rectangular input signal. It appeared that for the achievement of high efficiency, it is important to control harmonics at the output even inverse to class-F. Such an amplifier delivers the high device drain efficiency of a switched amplifier at class-A gain and, consequently, PAE is increased. We will show that this amplifier operates at reduced drain supply voltage and reduced negative gate-to-source voltage peaks. Furthermore, intermodulation distortion at saturation is also low.

II. Amplifier Concept

Fig. 1(b) illustrates gate and drain voltage and current waveforms and the dynamic load line of such a rectangularly driven class-A harmonic-control amplifier (rHCA). For the following discussion, we assume an FET with idealized characteristics. To prevent harmonics from reaching the fundamental-frequency load resistance, a harmonic load, which presents a short circuit at odd harmonics (except the first) and an open circuit at even harmonics, is used. Consequently, drain current becomes rectangular and drain-to-source voltage half-sinusoidal. Using the fundamental-frequency Fourier series components of drain current and voltage, output power can be determined to be

$$\begin{aligned} P_{\mathrm{OUT}} &= \frac{1}{2} I_D(1) \cdot V_{\mathrm{DS}}(1) \\ &= \frac{I_m (V_{\mathrm{DS}m} - V_K)}{2\pi} \\ &= P_{\mathrm{OUT,F}} \\ &= \frac{4}{\pi} P_{\mathrm{OUT,A}} \end{aligned} \tag{2}$$

which is as high as for class-F and about 1 dB larger than for classical class-A. The knee voltage V_K separates device ohmic from saturation region. With the dc input power

$$P_{\mathrm{DC}} = I_{D0} \cdot V_{\mathrm{DS0}} = \frac{I_m}{2\pi} [V_{\mathrm{DS}m} + (\pi - 1) V_K] \tag{3}$$

drain efficiency can be calculated being

$$\eta_D = \frac{P_{\mathrm{OUT}}}{P_{\mathrm{DC}}} = \frac{V_{\mathrm{DS}m} - V_K}{V_{\mathrm{DS}m} + (\pi - 1) V_K} = \kappa. \tag{4}$$

κ expresses the influence of V_K on efficiency and, for zero knee voltage, drain efficiency reaches 100%. Comparing input and output power of the rHCA with those of a classical class-A amplifier with sinusoidal input voltage, the gain can be expressed as

$$G = \frac{P_{\mathrm{OUT}}}{P_{\mathrm{IN}}(1)} = \frac{\frac{4}{\pi} P_{\mathrm{OUT,A}}}{\left(\frac{4}{\pi}\right)^2 P_{\mathrm{IN,A}}} = \frac{\pi}{4} G_{\mathrm{A}}. \tag{5}$$

This is only about 1 dB less than classical class-A gain and about 3.9 dB larger than class-F gain where half of the input signal is lost [see Fig. 1(a)]:

$$G_{\mathrm{F}} = \frac{P_{\mathrm{OUT,F}}}{P_{\mathrm{IN,F}}} = \frac{\frac{4}{\pi} P_{\mathrm{OUT,A}}}{4 P_{\mathrm{IN,A}}} = \frac{1}{\pi} G_{\mathrm{A}}. \tag{6}$$

TABLE I
Comparison of Calculated Important Amplifier Parameters of a Class-F Amplifier and an rHCA Using an Ideal FET with Zero Knee Voltage. Output Power P_{OUT}, Drain Efficiency η_D, Gain G, Maximum Drain-to-Source Voltage $V_{\mathrm{DS,max}}$, and Drain-to-Source Supply Voltage V_{DS0} Are the Abbreviations in Use

	Class F	rHCA
P_{OUT}	$\frac{4}{\pi}$ (+1.05 dB)	$\frac{4}{\pi}$ (+1.05 dB)
η_D	100 %	100 %
G	$\frac{1}{\pi}$ (-4.97 dB)	$\frac{\pi}{4}$ (-1.05 dB)
$V_{DS,max}$	$V_{BR} + 2V_P$	$V_{BR} + V_P$
V_{DS0}	$\frac{1}{2}V_{DSm}$	$\frac{1}{\pi}V_{DSm}$

As already mentioned, an increased gain increases PAE, especially for power devices where the available gain is relatively low.

Due to the half-sinusoidal drain-to-source voltage waveform, drain dc supply voltage is reduced to

$$V_{\mathrm{DS0}} = \frac{1}{\pi} [V_{\mathrm{DS}m} + (\pi - 1) V_K]. \tag{7}$$

For zero knee voltage and equal maximum drain-to-source voltage $V_{\mathrm{DS}m}$, drain supply voltage of the rHCA is only 64% of the class-F value. This concept-dependent advantage becomes important in combination with a handheld terminal, as it leads to a reduction of mass and size of its battery.

Finally, as in class-F operation the device is biased at its input at pinchoff V_P, gate-to-source voltage reaches values of twice the pinchoff voltage [see Fig. 1(a)]. This highly negative voltage stresses the gate due to reverse currents and gate breakdown, which may reduce amplifier reliability [13], [14]. The rHCA does not have gate-to-source voltage below V_P to deliver the same output power. In other words, as the upper limit of drain-to-source voltage $V_{\mathrm{DS,max}}$, where gate to drain breakdown V_{BR} occurs, is about $|V_P|$ higher for the rHCA

$$V_{\mathrm{DS,max}} = V_{\mathrm{BR}} + V_P \tag{8}$$

dc supply voltage can be increased, which results in higher output power.

The calculated performance of the most interesting amplifier parameters of class-F and the rHCA concept is summarized in Table I under the assumption of zero knee voltage. Output power and gain are given relatively to classical class-A values.

To generate the desired rectangular input signal, a pulse-forming driver stage has to be foreseen. This driver amplifier operates at an overdriven class-B mode, and gain loss and gate stress now appear in this stage. Fortunately, the driver stage operates already at much lower RF-power level than the power stage, permitting proper load-impedance selection for drain saturation and, therefore, avoiding any gate stress. Due to the high gain of the power stage, the reduction of overall efficiency of the two-stage amplifier due to the gain loss in the driver stage is kept within reasonable limits.

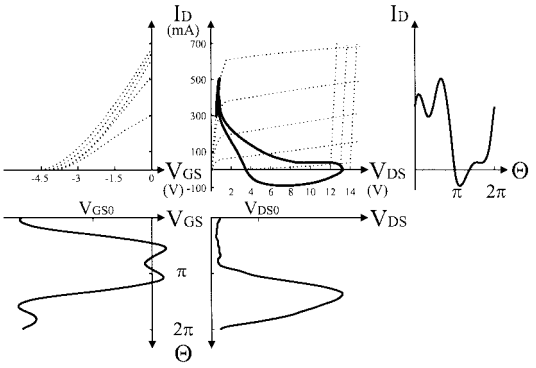

Fig. 2. Simulated input and output characteristics, gate and drain voltage and current waveforms, and dynamic load line of the FET TC6519 (Thomson) at rHCA operation.

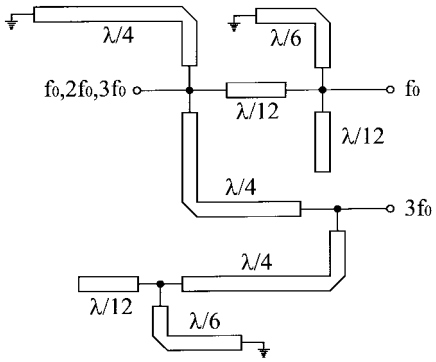

Fig. 3. Frequency-diplexing network. Lengths of transmission lines and stubs are given in wavelengths of fundamental frequency.

TABLE II
COMPARISON OF MEASURED AMPLIFIER PARAMETERS AND PERFORMANCE OF rHCA, INVERSE CLASS-F AMPLIFIER, AND CLASS-F AMPLIFIER WITH TC6519 OF THOMSON AT 1.6175 GHz. $\arg(\Gamma(2f_0))$ AND $\arg(\Gamma_L(3f_0))$ ARE THE ARGUMENTS OF SECOND AND THIRD HARMONIC-LOAD REFLECTION COEFFICIENTS OF THE OUTPUT MATCHING NETWORKS AND I_{D0} IS THE MEDIUM DRAIN CURRENT

Amplifier Concept		rHCA	Inv. Class F	Class F
	Units			
$\arg(\Gamma_L(2f_0))$	°	124	124	-178
$\arg(\Gamma_L(3f_0))$	°	-158	-158	120
V_{DS0}	V	4.75	4.75	6.1
I_{D0}	mA	181	181	128
P_{OUT}	dBm	28.2	28.1	27.8
G	dB	15.2	15.1	11.4
η_D	%	77	76	77
η_{PA}	%	75	73	71

III. AMPLIFIER DESIGN

To efficiently design such switched-type microwave amplifiers, we generated reliable transistor models, which precisely describe the FETs' pinchoff behavior and transition from ohmic to saturation region [15]. A modified TriQuint's Own model [16] seems to be optimum for this purpose in the light of performance at limited complexity.

Fig. 2 shows simulated gate and drain pulse forms and the dynamic load line of the power device (Thomson TC6519) obtained from harmonic-balance simulations. For simplicity of the final circuit design, the rectangular input signal is approximated by the fundamental frequency, and the right portion of third harmonic and at gate and drain harmonics are controlled only up to the third. To cut the negative-input voltage ripple, the device is biased at class-A near class-AB. As expected from theory, drain-to-source voltage is half-sinusoidal and drain current is an approximated rectangle. It has to be noted that at the drain neither an open circuit at second, nor a short circuit at third harmonic is optimum (see Table II). On the one hand, bond inductances and capacitances of the device package and, on the other hand, the intrinsic drain-to-source capacitance cause a shift of these optimum harmonic terminations. The simulated performance with ideal lossless matching networks is 28.7-dBm output power, 16.4-dB gain, and 80% PAE at 1.6175 GHz. The finite steepness of the input signal waveform increases the duty cycle and causes the drain current to flow during more than half of the time period (see Fig. 2). Therefore, losses occur inside the device due to an overlap of nonzero drain current and nonzero drain-to-source voltage. In our simulations, a relatively large portion of third harmonic-input signal ($P_{\mathrm{IN}}(3f_0) = P_{\mathrm{IN}}(f_0) - 2.4$ dB) was necessary to optimize the signal waveforms and, consequently, device drain efficiency.

For the optimization of the rHCA power stage, it is desirable to independently control fundamental frequency and third harmonic-input signals. Therefore, both signal components have to be separated from each other by an appropriate filtering network in the driver stage. Such a harmonic-frequency-diplexing circuit is illustrated in Fig. 3. The lengths of transmission lines and stubs are indicated in wavelengths of fundamental frequency (1.6175 GHz). At the fundamental-frequency output, an open-circuit stub of 1/12 wavelength in parallel with a short-circuit stub of 1/6 wavelength is used to achieve a short circuit at the third harmonic and an open circuit at the fundamental frequency. This open circuit at the fundamental frequency does not influence the behavior of the circuit at the fundamental frequency, but the short circuit at the third harmonic is transformed by a 1/12-wavelength line to an open circuit at the input. In the other branch, an open-circuit stub of 1/12 wavelength in parallel with a short-circuit stub of 1/6 wavelength is used to achieve an open circuit at fundamental frequency and a short circuit at the third harmonic again. These impedances are transformed by a quarter-wave transformer, connected to the third harmonic output, to a short circuit at the fundamental frequency and an open circuit at the third harmonic. This short circuit at the fundamental frequency is transformed by another quarter-wave transformer to an open circuit at the input. Additionally, the input is short circuited for all even harmonics by a short-circuited quarter-wave stub. Based on this circuit, matching networks for the driver amplifier output could be constructed with independent impedance-tuning possibilities for fundamental and third harmonic frequency, respectively.

After separation of fundamental frequency and third harmonic, magnitude and phase relation of both signal components are controlled using variable attenuators and a variable

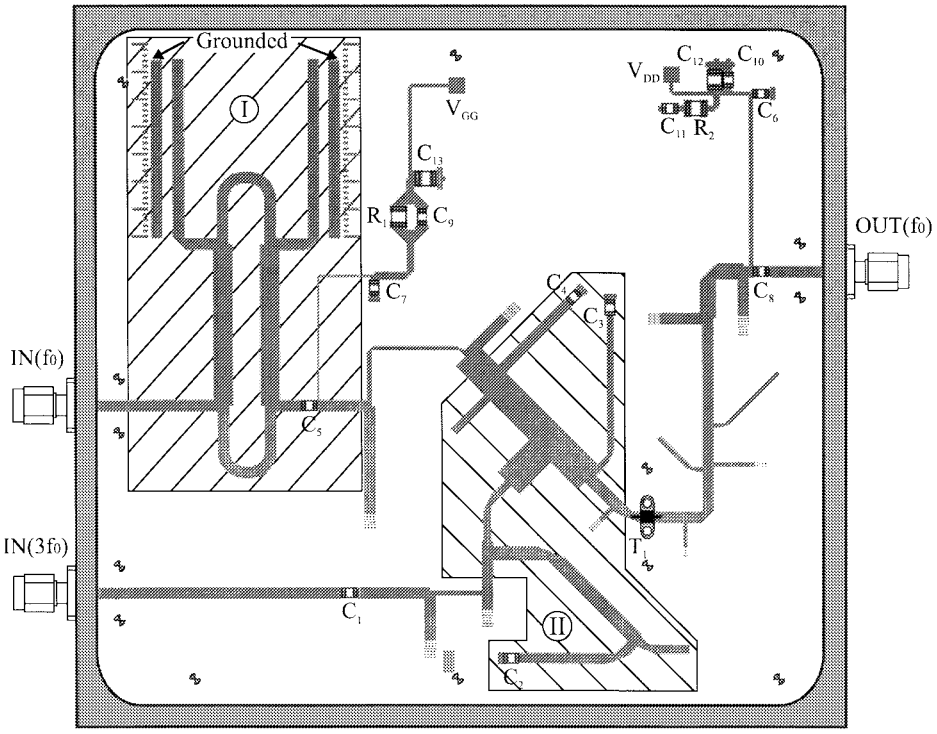

Fig. 4. Layout of final rHCA power stage. The hybrid phase shifter (I) and the frequency-diplexing network (II) are identified by hatched areas.

phase shifter within an interstage tuning network. Afterwards, they are combined in the power stage using the same diplexing network. Fig. 4 shows the layout of the power-amplifier stage with this frequency-diplexing circuit at the gate and with tuning possibilities for all source and load impedances. For the final two-stage design without external tuning elements, the phase shifter at fundamental-frequency input (which is based on a branch-line hybrid coupler) is used to adjust the optimum phase relation of both harmonic-input signals.

IV. Single-Stage Performance

Both amplifier stages needed only little tuning for optimum operation. Measurements on the power stage were performed using the combination of overdriven driver stage and interstage tuning network, which acted as a signal source for fundamental frequency and third harmonic. In the operating frequency range from 1.61 to 1.625 GHz, output power of the rHCA power stage is larger than 28.1 dBm, gain is 15.1 dB, and PAE is 74% as a minimum (see Fig. 5 and Table II). This is in good agreement with our simulation results with real matching structures.

For comparison with conventional class-F, we constructed such an amplifier using the same device as for the rHCA, but with different harmonic source and load terminations (see Table II). At center frequency ($f_0 = 1.6175$ GHz), the rHCA demonstrates an increased gain of 3.8 dB at the same drain efficiency, which results in a 4% higher PAE. Output power is also about 0.4 dB larger. Finally, the drain supply voltage is 4.75 V, about 1.35 V lower than for the class-F power stage.

Optimum fundamental frequency to third harmonic-input power ratio was determined to be 9 dB, which is much larger

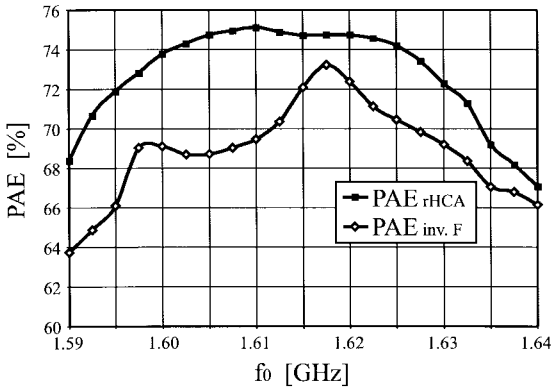

Fig. 5. Comparison of measured PAE over frequency of the power stage at rHCA and inverse class-F operation.

than the simulated value of 2.4 dB. It turned out that the real FET produces more third harmonic than predicted at its input itself, which can be used to perform input pulse forming when terminated with the right phase at the input.

Measurements on the power amplifier without any third harmonic-input power, but with an optimum tuned variable short at its third harmonic input, indicated only about 2%–6% lower PAE in the operating frequency range at almost the same output power and gain (see Fig. 5). In accordance with our notation, we call this kind of amplifier sinusoidally driven harmonic-control amplifier or inverse class-F amplifier at class-A near class-AB bias. Table II gives a comparison of measured performance of all three amplification modes.

Two-tone measurements were performed on the inverse class-F amplifier to determine its intermodulation distortion characteristic. In Fig. 6, third- and fifth-order signal-to-

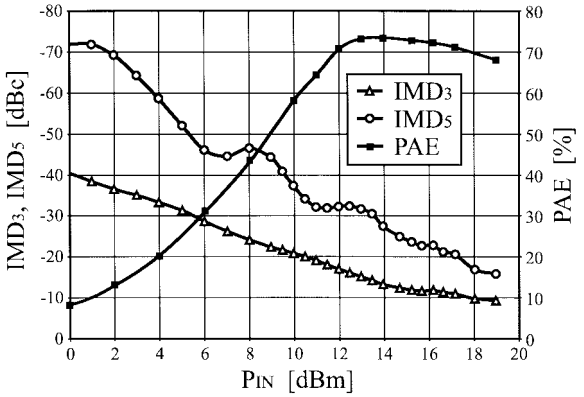

Fig. 6. Measured single-carrier PAE at $f_0 = 1.6175$ GHz and third- and fifth-order signal-to-intermodulation ratio (IMD_3, IMD_5) at two-tone stimuli ($f_1 = 1.615$ GHz, $f_2 = 1.62$ GHz) over the sum input power P_{IN} of the power stage at inverse class-F operation.

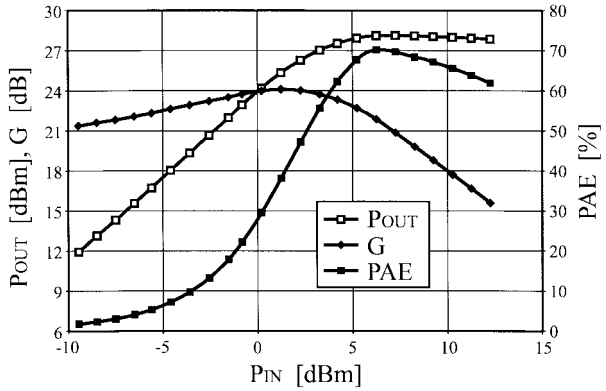

Fig. 7. Measured output power P_{OUT}, gain G, and overall PAE over input power P_{IN} of the two-stage rHCA at $f_0 = 1.6175$ GHz.

intermodulation ratio and single-carrier PAE are drawn over the sum input power. At optimum single-carrier input power IMD_3 is -16 dBc, whereas $\mathrm{IMD}_3 = -20$ dBc at an input power level where the single-carrier PAE is still 61%. For all input power levels, fifth-order intermodulation is much less than third-order intermodulation.

V. Two-Stage rHCA Performance

After determination of optimum fundamental and third harmonic-input power ratio of the rHCA power stage, the driver amplifier was tuned to produce exactly these output signals. The appropriate phase relation of both harmonic signals could be adjusted with the variable phase shifter of the power stage. In the following, we present the performance of this two-stage rHCA.

Output power, gain, and overall PAE over input power are shown in Fig. 7. Due to a gate bias of the driver stage at real class-B (meaning where the drain current is zero for zero input signal), overall gain is not constant for small input signals. A slightly increased (less negative) gate-to-source voltage linearizes the amplifier for these input power levels. At optimum input power, the two-stage amplifier operates about 2.5 dB in gain compression (calculated from its maximum gain level) and delivers 28.1-dBm output power, 21.4-dB gain, and

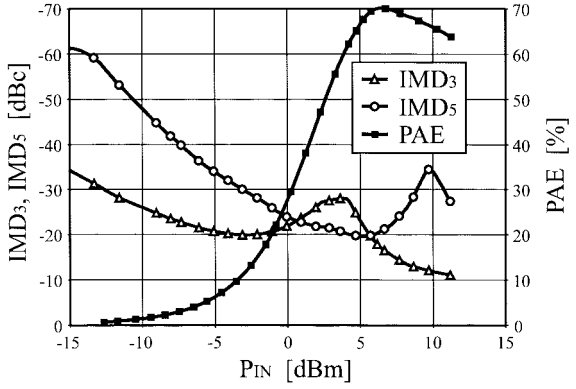

Fig. 8. Measured single-carrier overall PAE at $f_0 = 1.6175$ GHz and third- and fifth-order signal-to-intermodulation ratio (IMD_3, IMD_5) at two-tone stimuli ($f_1 = 1.615$ GHz, $f_2 = 1.62$ GHz) over the sum input power P_{IN} of the two-stage rHCA.

70% PAE at 1.6175 GHz. At the amplifier output, second and third harmonics are suppressed about -53 and -31 dB below the carrier, respectively. The reduction of PAE at increasing input power levels is partially caused by the gain reduction of the power stage and by an increasing malposition of phase relation of both harmonic-input signals of the rHCA power stage.

Finally, Fig. 8 presents the results of two-tone measurements on the two-stage amplifier over input power. At an input power level close to the single-carrier optimum, third- and fifth-order signal-to-intermodulation ratios are both -20 dBc. At reduced input power, third-order intermodulation products lie about 28 dB below the carrier, and fifth-order intermodulation distortion is predominating with -20 dBc. At this input power level, single-carrier PAE is 62%.

VI. Summary

We demonstrated that rectangular pulse shaping at the input and inverse class-F harmonic termination at the output of a class-A harmonic-control amplifier results in increased gain at the same drain efficiency and, therefore, increased PAE, as compared with class-F. Due to half-sinusoidal drain-to-source voltage pulse shaping, drain supply voltage of an rHCA is up to 1/3 lower at the same output power level. This is convenient for handheld terminals, as the number of battery cells can be reduced. Further advantages arise from the fact that due to a marked reduction of negative input voltage peaks and gate reverse currents amplifier reliability is improved. The realization of such an rHCA and a class-F amplifier at *L*-band confirms these advantages.

References

[1] G. Collinson and C. W. Suckling, "Effects of harmonic terminations on power and efficiency of GaAs HBT power amplifiers at 900 MHz," in *Dig. Inst. Elect. Eng. Colloq. Solid-State Power Amplifiers*, London, U.K., Dec. 1991, pp. 12/1–12/5.

[2] L. C. Hall and R. J. Trew, "Maximum efficiency tuning of microwave amplifiers," in *IEEE MTT-S Int. Microwave Symp. Dig.*, Boston, MA, 1991, pp. 123–126.

[3] S. Toyoda, "High-efficiency single and push-pull power amplifiers," in *IEEE MTT-S Int. Microwave Symp. Dig.*, Atlanta, GA, 1993, pp. 277–280.

[4] ——, "High efficiency amplifiers," in *IEEE MTT-S Int. Microwave Symp. Dig.*, San Diego, CA, 1994, pp. 253–256.
[5] ——, "High efficiency amplifier using rectangular waveform," in *IEEE MTT-S Int. Microwave Symp. Dig.*, Orlando, FL, 1995, pp. 705–708.
[6] M. Maeda, H. Masato, H. Takehara, M. Nakamura, S. Morimoto, H. Fujimoto, Y. Ota, and O. Ishikawa, "Source second-harmonic control for high efficiency power amplifiers," *IEEE Trans. Microwave Theory Tech.*, vol. 43, pp. 2952–2958, Dec. 1995.
[7] A. Iso, Y. Dooi, S. Kobayakawa, T. Miniwa, and N. Okubo, "A highly efficient, S-band, 100-W linear GaAs FET power amplifier for mobile communications satellites," in *41st Congr. Int. Astronautical Federation*, Dresden, Germany, Oct. 1990.
[8] C. Duvanaud, P. Bouysse, S. Dietsche, J. M. Nebus, J. M. Paillot, and D. Roques, "A design method for highly efficient power amplifiers: Application to class F amplifiers," *Int. J. Microwave Millimeter-Wave Computer-Aided Eng.*, vol. 6, pp. 288–293, 1996.
[9] S. Bouthillette and A. Platzker, "High efficiency L-band variable output power amplifiers for use in communication systems," in *IEEE MTT-S Int. Microwave Symp. Dig.*, San Francisco, CA, 1996, pp. 563–566.
[10] B. D. Geller and P. E. Goettle, "Quasi-monolithic 4-GHz power amplifiers with 65-percent power-added efficiency," in *IEEE MTT-S Int. Microwave Symp. Dig.*, New York, NY, 1988, pp. 835–838.
[11] J. Staudinger and G. Norris, "The effect of harmonic load terminations on RF power amplifier linearity for sinusoidal and $\pi/4$ DQPSK stimuli," in *IEEE MTT-S Int. Topical Symp. Technol. Wireless Applicat.*, Vancouver, B.C., Canada, Feb. 1996, pp. 23–28.
[12] B. Ingruber, W. Pritzl, and G. Magerl, "High efficiency harmonic control amplifier," in *IEEE MTT-S Int. Microwave Symp. Dig.*, San Francisco, CA, 1996, pp. 859–862.
[13] N. Constantin and F. M. Ghannouchi, "GaAs FET's gate current behavior and its effects on RF performance and reliability in SSPA's," *IEEE Trans. Microwave Theory Tech.*, vol. 43, pp. 2918–2925, Dec. 1995.
[14] J. V. DiLorenzo and D. D. Khandelwal, *GaAs FET Principles and Technology*. Norwood, MA: Artech House, 1982.
[15] B. Ingruber, D. Smely, and G. Magerl, "Fully automatic GaAs FET measurement and parameter extraction for large-signal modeling," in *Dig. 4th Int. Workshop Integrated Nonlinear Microwave Millimeterwave Circuits*, Duisburg, Germany, Oct. 1996, pp. 162–167.
[16] A. McCamant, G. McCormac, and D. Smith, "An improved GaAs MESFET model for SPICE," *IEEE MTT Trans. Microwave Theory Tech.*, vol. 38, pp. 822–824, June 1990.

Bernhard Ingruber (S'98) was born in Lienz, Austria, on October 16, 1966. He received the Dipl.-Ing. degree in electrical engineering and the Dr.Techn. degree from the Vienna University of Technology, Vienna, Austria, in 1992 and 1998, respectively.

Upon graduation, he joined the Austrian Research Center Seibersdorf, where he was engaged in a comparative study of existing safety standards of human exposure to microwave radiation. Since 1994, he has been a Research Assistant at the Vienna University of Technology. In 1994, he joined the Department of Communications and Radio-Frequency Engineering and, since 1998, he has been with the Department of Electronic Design and Measurement Techniques. He is involved in the analysis, design, and testing of high-efficiency and high-linearity microwave power amplifiers for handheld terminals for mobile-communication systems.

Josef Baumgartner, photograph and biography not available at the time of publication.

Dieter Smely received the Dipl.-Ing. degree in electrical engineering from the Vienna University of Technology, Vienna, Austria, in 1997 and is currently working toward the Ph.D. degree.

Since 1996, he has been a Research Assistant at the Vienna University of Technology. In 1996, he joined the Department of Communications and Radio-Frequency Engineering and, since 1998, he has been with the Department of Electronic Design and Measurement Techniques, where he is responsible for the design of high-precision microwave test fixtures and computer-controlled microwave measurements. In addition, he specializes in GaAs MESFET models. He is currently engaged in the development of high-power solid-state amplifiers.

Martin Wachutka (S'92) was born in Opponitz, Austria, on September 15, 1970. He received the Dipl.-Ing. degree in electrical engineering from the Vienna University of Technology, Vienna, Austria, in 1996.

From 1996 to 1997, he was a Research Assistant in the Department of Communications and Radio-Frequency Engineering, Vienna University of Technology. In 1998, he joined UTA Telecom AG, Vienna, Austria.

Gottfried Magerl (M'78) was born in Vienna, Austria, on August 16, 1947. He received the Dipl.-Ing. and Dr.Techn. degrees from the Vienna University of Technology, Vienna, Austria, in 1972 and 1975, respectively.

Since 1973, he has been with the Department of Communications and Radio Frequency Engineering, Vienna University of Technology. In 1981, he was appointed Academic Lecturer (Universitätsdozent). In 1990, he became a University Professor of microwave engineering, and recently became Head of the Department of Electronic Design and Measurement Techniques. He spent the 1981–1982 academic year and the summer months of 1984 and 1986 at the University of Chicago and University of Michigan, East Lansing, where he constructed high-resolution infrared (IR) spectrometers based on the microwave modulation of CO_2 and CO lasers via the electrooptic effect in CdTe. His interest in the application of electromagnetic radiation to noncontacting measurement techniques led to the development of a road-condition sensing microwave radar and to extensive work on physics and optimization of narrow-band atomic line filters. His current research interests concentrate on the development of highly efficient linear microwave power amplifiers for mobile communications.

Felix A. Petz received the B.S. degree in electronics from the Engineering School, Graz, Austria, in 1966, and the M.S. degree in physics from the University of Munich, Munich, Germany, in 1977.

He started his professional career working for six years in the computer industry (field engineering and optical pattern recognition), and continued working for another six years in the microwave semiconductor field (monolithic microwave integrated circuit (MMIC) and solid-state power-amplifier (SSPA) development) in Germany and the U.S. He dedicated the following five years to system engineering for space-based remote-sensing instruments (ERS-1 and SIR-C/X-SAR synthetic aperture radar). He has been with the European Space Agency (ESA-ESTEC), Noordwijk, The Netherlands, for nine years, where he is currently responsible for the definition and management of R&D contracts for Earth observation and mobile-communication payload electronics (SAR 2000, Inmarsat P21, and various subsystems).